Available online at www.sciencedirect.com
ScienceDirect
Trans. Nonferrous Met. Soc. China 25(2015) 2279−2284
Transactions of Nonferrous Metals Society of China
www.tnmsc.cn

Effect of Fe_2O_3 on non-isothermal crystallization of $CaO−MgO−Al_2O_3−SiO_2$ glass

Qing-chun YU[1,2], Chun-pei YAN[1,2], Yong DENG[1,2], Yue-bin FENG[3], Da-chun LIU[1,2], Bin YANG[1,2]

1. National Engineering Laboratory of Vacuum Metallurgy,
Key Laboratory of Nonferrous Metal Vacuum Metallurgy of Yunnan Province,
Faculty of Metallurgical and Energy Engineering,
Kunming University of Science and Technology, Kunming 650093, China;
2. State Key Laboratory of Complex Nonferrous Metal Resources Clear Utilization,
Kunming University of Science and Technology, Kunming 650093, China;
3. Faculty of Science, Kunming University of Science and Technology, Kunming 650500, China

Received 9 September 2014; accepted 23 January 2015

Abstract: The crystallization behavior and kinetics of $CaO−MgO−Al_2O_3−SiO_2$ (CMAS) glass with the Fe_2O_3 content ranging from zero to 5% were investigated by differential scanning calorimetry (DSC). The structure and phase analyses were made by Fourier transform infrared spectroscopy (FT-IR) and X-ray diffraction (XRD). The experiment results show that the endothermic peak temperature about 760 °C is associated with transition and the exothermic peak temperature about 1000 °C is associated with crystallization. The crystallization peak temperature decreases with increasing the Fe_2O_3 content. The crystallization mechanism is changed from two-dimensional crystallization to one-dimensional growth, and the intensity of diopside peaks becomes stronger gradually. There is a saltation for the crystallization temperature with the addition of 0.5% Fe_2O_3 due to the decomposition of Fe_2O_3. Si—O—Si, O—Si—O and T—O—T (T=Si, Fe, Al) linkages are observed in $Fe_2O_3−CaO−MgO−Al_2O_3−SiO_2$ glass.
Key words: $CaO−MgO−Al_2O_3−SiO_2$ glass; Fe_2O_3; diopside; crystallization; kinetics

1 Introduction

The glass-ceramics based on $CaO−MgO−Al_2O_3−SiO_2$ (CMAS) quaternary system, which are mainly produced from inexpensive natural or synthetic materials, such as fly ash, blast furnace slag, basalt, oil shale, granite and tuff, have received increasing attention during the past few decades. Blast furnace (BF) slag is one of the most abundant solid by-products in steel plants. Currently most of BF slag in China has been used for cement manufacturing and civil engineering, and the remaining amount is deposited in landfill. BF slag, which is mainly composed of CaO, SiO_2, Al_2O_3 and MgO, is the excellent raw material for the production of glass-ceramics [1]. Recycling these slags is necessarily beneficial not only for economy, but also for environmental friendly steel plants.

Glass-ceramics were usually prepared by controlling nucleation and crystallization. Lots of researches about preparation of glass-ceramics from solid waste have been done [2−4]. Some additives such as Cr_2O_3, TiO_2, CaF_2, MgO and CaO [5,6] used as fluxes or nucleation agents were reported. Recently, the effect of MgO on the glass-ceramics crystallization and structure was investigated [7]. With increasing MgO addition, the glass ceramic crystallization kinetics under non-isothermal conditions was changed from bulk crystallization to surface crystallization, and new crystal phases of $Ca_2MgSi_2O_7$ and SiO_2 were induced. Fe_2O_3 played an important role on nucleation or crystallization behavior as well as the heat-treated time. LI et al [8] studied the effect of Fe_2O_3 on the crystallization kinetics of Baiyunebo tailing. It was found that Fe_2O_3 provided the core of nucleation for the consequent precipitation of augite crystals, and could effectively mend the Si—O net

Foundation item: Projects (51264023, 51364020, U1202271) supported by the National Natural Science Foundation of China; Project (IRT1250) supported by the Program for Innovative Research Team in University of Ministry of Education of China; Project (2014HA003) supported by the Science and Technology Leading Talent of Yunnan Province, China
Corresponding author: Qing-chun YU; Tel: +86-871-65161583; E-mail: yqcy@163.com
DOI: 10.1016/S1003-6326(15)63842-0

structure when the Fe_2O_3 content reached 13.3%. ALIZADEH et al [9] researched the effect of Fe_2O_3 on the sinterability and machinability of Fe_2O_3-doped glass-ceramics in the system $MgO−CaO−SiO_2−P_2O_5$. ROMERO et al [10] studied the influence of Fe_2O_3 content on the main crystalline phase of $MgO−CaO−SiO_2−Fe_2O_3$ glass-ceramic and the size of franklinite. KARAMANOV et al [11] prepared glass-ceramic from two hazardous industrial wastes: mud (goethite and jarosite) originating from the zinc hydro-metallurgical process and electric arc furnace dust, and discussed the influence of Fe^{3+}/Fe^{2+} ratio on the crystallization. WANG et al [12] investigated the nucleation mechanism, crystallization behavior and infrared radiation properties of $MgO−Al_2O_3−SiO_2$ system glass when Fe_2O_3 was doped.

Fe_2O_3 is unavoidable in solid wastes, especially in BF slags and steel slags. It is significant to research the glass-ceramics containing Fe_2O_3. The aim of this work is to investigate the effect of Fe_2O_3 on the structure and the crystallization behavior of CMAS quaternary system glass, as well as the crystallization kinetics, and to take advantage of Fe_2O_3 to the production of glass-ceramic from BF slag or steel slag.

2 Experimental

2.1 Sample preparation

Five basic glass samples, with chemical compositions presented in Table 1, were prepared by mixing SiO_2, Al_2O_3, MgO, CaO and Fe_2O_3. The melting of these glass samples was carried out in corundum crucible using a high temperature furnace with $MoSi_2$ heating element. The melts were kept at 1450 °C for 2 h, and were immediately poured on a pre-heated metallic mould with annealing at 500 °C for 2 h to obtain the basic glass samples.

Table 1 Chemical compositions of samples

Sample No.	Mass fraction/%				
	CaO	MgO	Al_2O_3	SiO_2	Fe_2O_3
1	21.000	15.000	10.000	54.000	−
2	20.895	14.925	9.950	53.730	0.500
3	20.790	14.850	9.900	53.460	1.000
4	20.580	14.700	9.800	52.920	2.000
5	20.370	14.550	9.700	52.380	3.000

2.2 Thermal measurements

Differential scanning calorimetry (DSC) analysis was made using a Netzsch STA 449F3 thermal balance from 200 to 1200 °C. The particle size of the basic glass samples ranged from 74 to 104 μm. The DSC profiles were automatically recorded at different heating rates. Based on the principle that the crystallization temperature varied with the heating rates, the activation energy of crystallization was calculated. The heating rates were selected as 5, 10, 15, and 20 °C/min.

2.3 Morphology and microstructure analysis

X-ray diffraction analysis (D/max−TTRⅢ, Rigaku Japan) was performed using a graphite monochromatic Cu K_α radiation. The X-ray patterns were obtained by measuring 2θ from 10° to 70° with a step size of 0.02°. Fine powders of the samples were mixed with KBr powders in a mass ratio of 1:100 and the mixtures were suppressed in a die to produce clear homogeneous disc. The basic glass samples were measured at room temperature in the wave number range of 2500−500 cm^{-1} using a Fourier transform infrared spectrometer (AVATAR, FT−IR360, ThermoNicolet, America).

3 Results and discussion

3.1 DSC Analysis

Figure 1 shows the DSC profiles of glass samples with different amounts of Fe_2O_3 at heating rates of 5, 10, 15, and 20 °C/min. It can be found that both the glass transition temperatures T_g and crystallization peak temperatures T_p decrease with increasing the Fe_2O_3 content. However, the trends of crystallization peak temperatures $T_{p,}$ as well as the endothermic peak shape and its intensity, are alike. It should be noted that the crystallization peak temperatures of Sample 2 at different heating rates decrease sharply which are even lower than those of Samples 3 and 4. The tendency can be seen from Table 2 which summarizes the important characteristics of DSC profiles from different samples as well as different heating rates. This can be explained by the transformation of Fe_2O_3 from Fe^{3+} to Fe^{2+} as follows:

$$Fe_2O_3 = 2FeO + 1/2O_2 \quad (1)$$

$$3Fe_2O_3 = 2Fe_3O_4 + 1/2O_2 \quad (2)$$

As was reported in Ref. [13], Fe^{2+} reduced the viscosity of glass, while Fe^{3+} was considered as an intermediate ion and might cause an opposite influence on the viscosity of glass. It could be conjectured that trace amount of Fe_2O_3 in CMAS quaternary system is decomposed and Fe^{3+} is changed into Fe^{2+}. With increasing the Fe_2O_3 content, the ratio of Fe^{3+}/Fe^{2+} and the viscosity increase. A saltation occurs for the crystallization peak temperature (T_p) with the addition of 0.5% Fe_2O_3.

3.2 Calculation of crystallization kinetics

The crystallization kinetics was determined by the DSC profiles at different heating rates. The activation energy of crystallization, E_a, was calculated from the

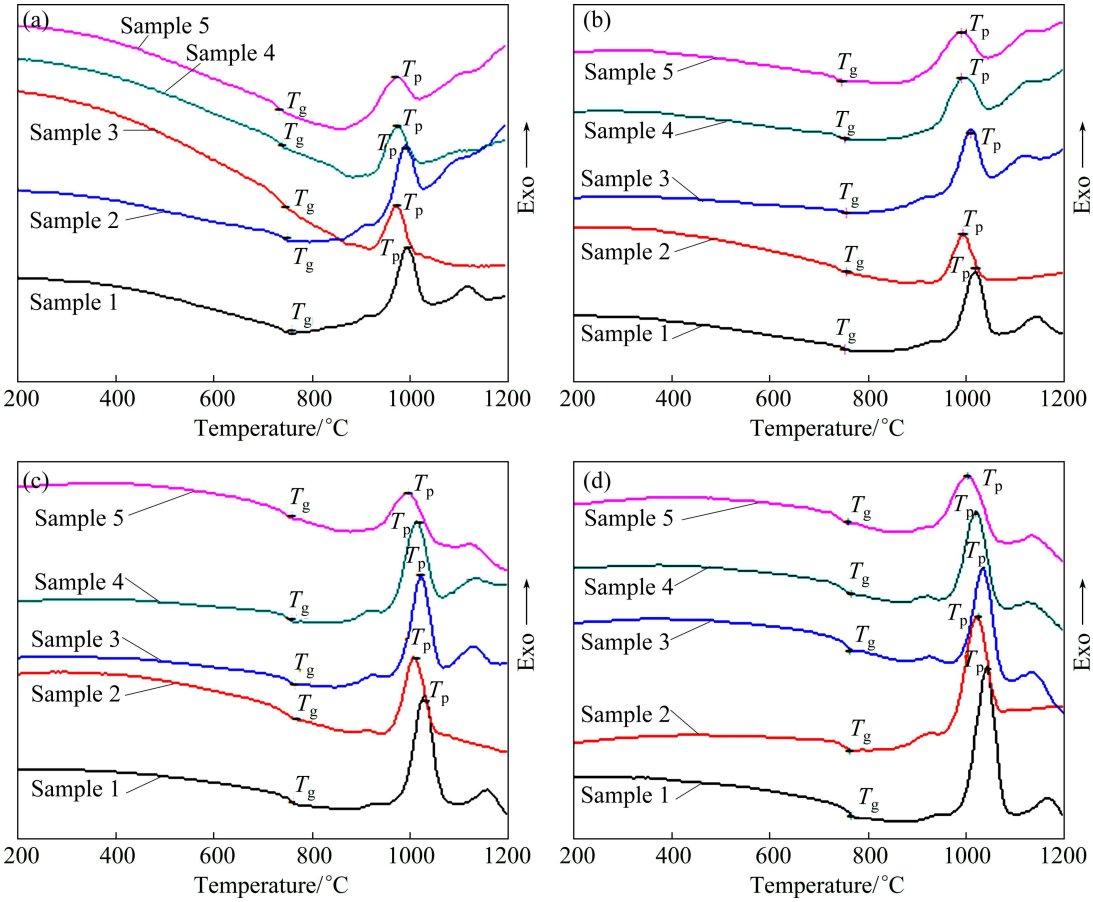

Fig. 1 DSC profiles of five glass samples at different heating rates: (a) 5 °C/min; (b) 10 °C/min; (c) 15 °C/min; (d) 20 °C/min

Table 2 Crystallization peak temperatures of different samples at different heating rates

Sample No.	Crystallization peak temperature/°C			
	5 °C/min	10 °C/min	15 °C/min	20 °C/min
1	994.4	1015.3	1026.5	1038.9
2	972.4	991.2	1004.5	1018.6
3	990.4	1008.1	1020.0	1030.6
4	975.6	997.8	1010.5	1017.0
5	969.9	986.6	992.2	999.5

exothermic DSC crystallization peak temperatures using the Kissinger equation as follows [14]:

$$\ln\left(\frac{T_p^2}{\alpha}\right)=\ln\left(\frac{E_a}{R}\right)+\frac{E_a}{RT_p}+C \tag{3}$$

where T_p is the crystallization peak temperature (K), α is the heating rate (K/s), E_a is the activation energy of crystallization (J/mol), R is the mole gas constant (8.314 J/(mol·K)), and C is a constant.

The plot of $\ln(T_p^2/\alpha)$ as a function of $1/T_p$ gives a straight line, and the slope takes the value of E_a/R. The Avrami constant n, describing the dimensionality of crystal growth, can be calculated by the Augis−Bennett equation as follows [14]:

$$n=\left(\frac{2.5}{\Delta T_{FWHM}}\right)\times\left(\frac{RT_p^2}{E_a}\right) \tag{4}$$

where ΔT_{FWHM} is the full width of the exothermic peak at the half maximum intensity. The crystallization mechanism can be determined from the Avrami constant n. The Avrami constant n close to 1, 2, 3, and 4 means one-dimensional growth, two-dimensional crystallization, three-dimensional growth (bulk crystallization), and homogeneous crystallization [15], respectively.

The plots of $\ln(T_p^2/\alpha)$ versus $1/T_p$ for all the samples are shown in Fig. 2. The activation energy of crystallization E_a and the Avrami constant n are listed in Table 3. It can be found that the activation energy of crystallization E_a with the addition of 0.5% Fe_2O_3 is the lowest. The maximum Avrami constant 1.96 means two-dimensional crystallization. With increasing the Fe_2O_3 content, the Avrami constant n decreases, and the crystallization mechanism is changed from two-dimensional crystallization to one-dimensional growth.

According to Dietzel's ionic field strength theory, McMILLAN [2] reported that when I ($I=z/r^2$, where z is

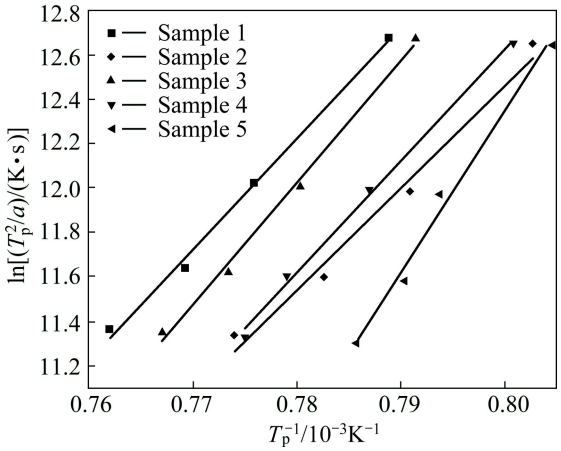

Fig. 2 Plots of $\ln(T_p^2/\alpha)$ versus $1/T_p$

Table 3 Activation energy (E_a) and Avrami constant (n) for crystallization

Sample No.	E_a/(kJ·mol^{-1})	n
1	416.97	1.95
2	384.64	1.96
3	454.78	1.84
4	418.67	1.71
5	602.79	0.81

the cation charge, and r is the radius of ion) was greater than 5 Å^{-2}, the metal ions formed nets in glass system; when I was less than 5 Å^{-2}, the metal ions were outside the nets; when I was equal to 5 Å^{-2}, the effect of metal ions was dependent on the concentration of monovalent or divalent metal ions in glass. If the concentration of monovalent or divalent metal ions in glass was high, it would fill the nets in glass system. Otherwise, it would do damage to the nets in glass system. The ionic field strengths of Fe^{2+} and Fe^{3+} were 3.65 and 7.32 Å^{-2}, respectively [16]. The ionic field strength of Fe^{2+} was less than 5 Å^{-2}. Fe^{2+} acted as net breakers in the anionic structure, and destroyed the [SiO_4] tetrahedron nets in glass system. Thus, the activation energy of crystallization and the crystallization peak temperature decreased. With increasing the Fe_2O_3 content, Fe^{3+} played a major role in mending nets and accumulation of [SiO_4] tetrahedron, thereby improving the viscosity and the oxidizing atmosphere. Thus, the activation energy of crystallization and the crystallization peak temperature increased.

3.3 Structure and FTIR analysis

Fourier transform infrared spectroscopy analysis of the basic glass samples was also conducted. As shown in Fig. 3, the absorption bands are divided into three parts. The first part in the range of 1200−850 cm^{-1} is the most intense broad band. This part is assigned to the stretching vibrations of Si — O — Si linkages in the [SiO_4] tetrahedron unit [17,18]. With respect to the aluminum coordination in glass structure, this broad band is in accordance with the infrared spectroscopy of potassium feldspar with [AlO_4] for the stretching vibration of Al — O — Al linkages. The band between 800 and 600 cm^{-1} is the second part, which shows the aggregation structure of glass, namely, the symmetric stretching vibrations of the tetrahedral structure including T—O—T (T=Si, Fe, Al) [19]. The third part starts at 600 cm^{-1}, and goes down at about 400 cm^{-1}. This group corresponds to the bending vibrations of O—Si—O linkages.

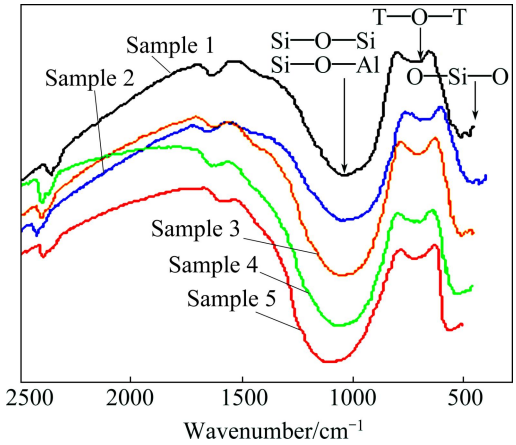

Fig. 3 FT-IR profiles of basic glass samples

In Fig. 3, the five profiles are similar with each other, but it can be noticed obviously that the plot of Sample 2 is wider than that of the other four samples in the range of 1200−850 cm^{-1}. This is in accordance with the change of crystallization peak temperature. Meanwhile, in the range of 800−600 cm^{-1}, it is found that the absorption peak shifts from high frequency to low frequency, and then to high frequency again. This confirms that the polymerization degree of T—O—T in Sample 2 is the lowest.

3.4 XRD analysis

Figure 4 shows the X-ray diffraction patterns of the basic glass samples nucleated at 800 °C for 2 h and crystallized at 1050 °C for 2 h. The main phases of diopside ($Ca(Mg,Al)(Si,Al)_2O_6$) and wollastonite-2M ($CaSiO_3$) are observed in Fig. 4. It can be noticed that, with increasing the Fe_2O_3 content, the intensity of diopside becomes stronger gradually. Sample 1 is amorphous as some of the diopside peaks are not visible clearly. As was reported in Ref. [20], the glass-ceramics based on diopside, with excellent mechanical properties, high abrasive resistance and good chemical resistance, were good candidates for decorative materials in construction field.

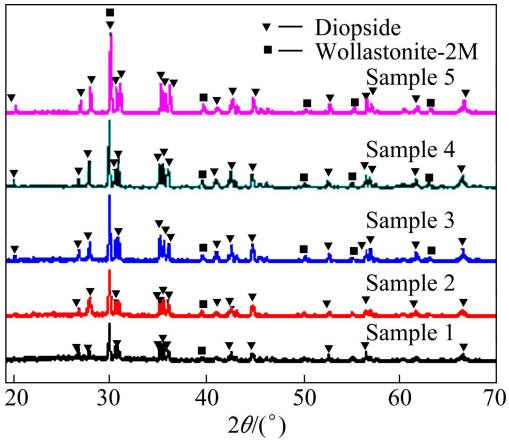

Fig. 4 XRD patterns of glass-ceramics samples

4 Conclusions

1) The endothermic peak temperature about 760 °C associated with transition and the exothermic peak temperature about 1000 °C associated with crystallization were found when the Fe_2O_3−CaO−MgO−Al_2O_3−SiO_2 basic glass was heated. With increasing the Fe_2O_3 content, the glass transition temperature T_g and crystallization temperature T_p decrease. There is a saltation with the addition of 0.5% Fe_2O_3 due to the decomposition of Fe_2O_3.

2) The general trend of the activation energy of crystallization with increasing the Fe_2O_3 content is down. Si—O—Si, O—Si—O and T—O—T (T=Si, Fe, Al) linkages are observed in Fe_2O_3−CaO−MgO−Al_2O_3−SiO_2 glass.

3) As the Fe_2O_3 content increases, the crystallization mechanism is changed from two-dimensional crystallization to one-dimensional growth, and the intensity of diopside peaks becomes stronger gradually.

References

[1] GAN lei, ZHANG Chun-xia, ZHOU Ji-cheng, SHANGGUAN Fang-qin. Continuous cooling crystallization kinetics of a molten blast furnace slag [J]. Journal of Non-Crystalling Solids, 2012, 358: 20−24.

[2] McMILLAN P W. Glass-ceramics [M]. 2nd ed. London: Academic Press, 1979: 231−263.

[3] EROL M, KUCUKBAYRAK S, MERCBOYU AE, OVECOGLU M L. Crystallization behavior of glasses produced from fly ash [J]. Journal of the European Ceramic Society, 2001, 21: 2835−2841.

[4] YILMAZ S, BAYRAK G, SEN S, SEN U. Structural characterization of basalt-based glass-ceramic coating [J]. Materials and Design, 2006, 27: 1092−1096.

[5] REZVANI M, EFTERKHARI-YEKTA B, SOLATI-HASHJIN M, MARGHUSSIAN V K. Effect of Cr_2O_3, Fe_2O_3 and TiO_2 nucleants on the crystallization behavior of SiO_2−Al_2O_3−CaO−MgO (R_2O) glass-ceramics [J]. Ceramics International, 2005, 31: 75−80.

[6] DUAN Ren-guan, LIANG Kai-ming, GU Shou-ren. Effect of changing TiO_2 content on structure and crystallization of CaO−Al_2O_3−SiO_2 glass system [J]. Journal of the European Ceramic Society, 1998, 18: 1729−1735.

[7] MA J, CHEN C Z, WANG D G, SHAO X, WANG C Z, ZHANG H M. Effect of MgO addition on the crystallization and in vitro bioactivity of glass ceramics in the CaO−MgO−SiO_2−P_2O_5 system [J]. Ceramics International, 2012, 38: 6677−6684.

[8] LI Bao-wei, DU Yong-sheng, ZHANG Xue-feng, JIA Xiao-lin, ZHAO Ming, CHEN Hua. Effects of iron oxide on the crystallization kinetics of baiyunebo tailing glass-ceramics [J]. Transactions of the Indian Ceramic Society, 2013, 2: 119−123.

[9] ALIZADEH P, YEKTA B E, GERVEI A. Effect of Fe_2O_3 addition on the sinterability and machinability of glass-ceramics in the system MgO−CaO−SiO_2−P_2O_5 [J]. Journal of the European Ceramic Society, 2004, 24: 3529−3533.

[10] ROMERO M, RINCON J M, ACOSTA A. Effect of iron oxide content on the crystallization of a diopside glass-ceramic glaze [J]. Journal of the European Ceramic Society, 2002, 22: 883−890.

[11] KARAMANOV A, PISCIELLA P, CANTALINI C, PELINO M. Influence of Fe^{3+}/Fe^{2+} ratio on the crystallization of iron-rich glasses made with industrial wastes [J]. Journal of the American Ceramic Society, 2000, 83: 3153−3157.

[12] WANG Shu-ming, KUANG Feng-hua, YAN Qing-zhi, GE Chang-chun, QI Long-hao. Crystallization and infrared radiation properties of iron ion doped cordierite glass-ceramics [J]. Journal of Alloys and Compounds, 2011, 509: 2819−2823.

[13] YANG Zhi-jie, LI Yu, CANG Da-qiang, DIAO Mei-ling, GUO Wen-bo. The influence of Fe^{2+} and Fe^{3+} on crystallization of CaO−Al_2O_3−SiO_2−MgO system glass-ceramic [J]. Materials Science and Technology, 2012, 20: 45−50. (in Chinese)

[14] KARAMANOV A, PISCIELLA P, PELINO M. The crystallisation kinetics of iron rich glass in different atmospheres [J]. Journal of the European Ceramic Society, 2000, 20: 2233−2237.

[15] SALAMA S N, SALMAN S M, DARWISH H. The effect of nucleating catalysts on crystallization characteristics of aluminosilicate glasses [J]. Ceramics Silikaty, 2002, 46(1): 15−23.

[16] ZHANG Lian-meng, HUANG Xue-hui, SONG Xiao-feng. Fundamentals of materials science [M]. Wuhan: Wuhan University of Technology Press, 2009. (in Chinese)

[17] ATALAY S, ADIGUZEL H I, ATALAY F. Infrared absorption study of Fe_2O_3−CaO−SiO_2 glass ceramics [J]. Materials Science and Engineering A, 2001, 304−306: 796−799.

[18] ELBATAL F H, MOENIS A A, YOUSRY M H. Preparation and characterization of some multicomponent silicate glasses and their glass−ceramics derivatives for dental applications [J]. Ceramics International, 2009, 35: 1211−1218.

[19] REDDY A A, GOELA A, TULYAGANOV D U, KAPOOR S, PRADEESH K, PASCUAL M J. Study of calcium–magnesium–aluminum–silicate (CMAS) glass and glass−ceramic sealant for solid oxide fuel cells [J]. Journal of Power Sources, 2013, 231: 203−212.

[20] MARQUES V M F, TULYAGANOV D U, AGATHOPOULOS S, FERRIRA J M F. Low termperature production of glass ceramics in the anorthite−diopside system via sintering and crystallization of glass powder compacts [J]. Ceramics International, 2008, 27: 661−668.

Fe_2O_3 对 $CaO-MgO-Al_2O_3-SiO_2$ 玻璃非等温析晶的影响

郁青春[1,2]，燕春培[1,2]，邓 勇[1,2]，冯月斌[3]，刘大春[1,2]，杨 斌[1,2]

1. 昆明理工大学 冶金与能源工程学院，真空冶金国家工程实验室，
云南省有色金属真空冶金重点实验室，昆明 650093；
2. 昆明理工大学 省部共建复杂有色金属资源清洁利用国家重点实验室，昆明 650093；
3. 昆明理工大学 理学院，昆明 650500

摘 要：采用差示扫描量热法(DSC)研究 Fe_2O_3 含量在 0~5%范围内的 $CaO-MgO-Al_2O_3-SiO_2$ (CMAS)玻璃的析晶行为及动力学。采用傅里叶红外光谱分析(FT-IR)和 X 射线衍射分析(XRD)研究其物相结构。结果表明：吸热峰温度 760 °C 为转变温度，放热峰温度 1000 °C 为析晶温度。随着 Fe_2O_3 含量的增加，析晶温度降低，析晶机理从二维析晶转变为一维生长，透辉石的衍射峰强度增强。由于 Fe_2O_3 的分解，Fe_2O_3 含量为 0.5%时析晶温度发生突变。$Fe_2O_3-CaO-MgO-Al_2O_3-SiO_2$ 玻璃中发现 Si—O—Si，O—Si—O 及 T—O—T (T=Si, Fe, Al)的联接结构。

关键词：$CaO-MgO-Al_2O_3-SiO_2$ 玻璃；Fe_2O_3；透辉石；析晶；动力学

(Edited by Mu-lan QIN)